

Evaluation of the pressure tensor and surface tension for molecular fluids with discontinuous potentials using the volume perturbation method

Guadalupe Jiménez-Serratos, Carlos Vega, and Alejandro Gil-Villegas

Citation: *J. Chem. Phys.* **137**, 204104 (2012); doi: 10.1063/1.4767375

View online: <http://dx.doi.org/10.1063/1.4767375>

View Table of Contents: <http://jcp.aip.org/resource/1/JCPSA6/v137/i20>

Published by the [American Institute of Physics](#).

Additional information on *J. Chem. Phys.*

Journal Homepage: <http://jcp.aip.org/>

Journal Information: http://jcp.aip.org/about/about_the_journal

Top downloads: http://jcp.aip.org/features/most_downloaded

Information for Authors: <http://jcp.aip.org/authors>

ADVERTISEMENT



**ACCELERATE COMPUTATIONAL CHEMISTRY BY 5X.
TRY IT ON A FREE, REMOTELY-HOSTED CLUSTER.**

[LEARN MORE](#)

Evaluation of the pressure tensor and surface tension for molecular fluids with discontinuous potentials using the volume perturbation method

Guadalupe Jiménez-Serratos,¹ Carlos Vega,² and Alejandro Gil-Villegas^{1,a)}

¹*Departamento de Ingeniería Física, División de Ciencias e Ingenierías Campus León, Universidad de Guanajuato, Colonia Lomas del Campestre, León 37150, Mexico*

²*Departamento de Química Física, Facultad de Ciencias Químicas, Universidad Complutense de Madrid, Ciudad Universitaria 28040, Madrid, Spain*

(Received 6 September 2012; accepted 30 October 2012; published online 26 November 2012)

In this article we apply the volume-perturbation method to systems of particles interacting via discontinuous potentials. We have found that an accurate Monte Carlo simulation protocol can be used in order to study properties of very general non-spherical systems with discontinuous potentials, such as chain molecules and spherocylinders with square-well interactions, and chain molecules with square-well and square-shoulder interactions. From the simulation results obtained for these systems we verify that: (1) the method reproduces the pressure as used in NPT simulations; (2) discontinuous infinite repulsive interactions give asymmetric contributions to the pressure when compression and expansion movements are used; however for finite interactions these contributions are symmetric; and (3) the pressure contributions preserve the additivity of the potential interactions. Density profiles and surface tension for subcritical conditions are accurately predicted. © 2012 American Institute of Physics. [<http://dx.doi.org/10.1063/1.4767375>]

I. INTRODUCTION

The evaluation of the surface tension in fluids using computer simulations has followed two routes, the mechanical method based on the Clausius virial theorem¹ and the thermodynamic method based on the relationship between pressure and the Helmholtz (or Gibbs) free energy.^{2,3} Surface tension is determined from the diagonal elements of the pressure tensor, and the thermodynamic pressure p is given by one third of the trace of this tensor. From elasticity theory we know that for a homogeneous system in thermodynamic equilibrium, the off-diagonal elements of the pressure tensor are null, whereas the diagonal elements become identical; then the pressure p is called the hydrostatic pressure.⁴

Both methods are neither independent nor they give alternative definitions of the surface tension.⁵ From a fundamental point of view, pressure arises as a consequence of the flux of momentum, a physical mechanism that can be decomposed into the different ways in which this flux takes place. There is a flux due to the momentum transported by the molecules, and there is another flux due to elastic collision between molecules.^{6,7} In this way, the Clausius virial theorem takes into account both mechanisms, being the first one the origin of the ideal gas contribution to the pressure. Collision between particles is due to the intermolecular forces acting between molecules, so the average of the virial $\mathbf{r} \cdot \mathbf{F}$ gives the non-ideal contribution to the pressure. The analysis of the flux of momentum can be done for homogeneous and inhomogeneous phases. In inhomogeneous systems, the diagonal elements of the pressure tensor are not equal, and the surface tension is due to this difference.

By using the theoretical framework developed by Zwanzig for perturbation theory in Statistical Mechanics,⁸ as well as previous computer simulation studies performed by Eppenga and Frenkel,⁹ Harismiadis *et al.*¹⁰ and Vörtler and Smith,¹¹ Jackson and de Miguel derived novel approaches to obtain the surface tension and the components of the pressure tensor using the test-area (TA)¹² and the volume-perturbation (VP) methods,¹³ respectively. Both methods have been extended to model interfacial properties of non-spherical and non-convex molecules^{14,15} and solid-fluid interfacial tension of spherical molecules adsorbed in slit-like pores.¹⁶ Other applications studied with these methodologies have been the surface tension of different models of water,^{17,18} vapor-liquid interfacial properties of diatomic molecules¹⁹ and fully flexible Lennard-Jones chain molecules.²⁰ Alternative methods to the TA and VP approaches have been proposed: the wandering interface,²¹ the expanded ensemble method,²² and more recently, the non-exponential method by Ghoufi and Malfreyet.²³

The temperature region of interest, potential range, and computational requirements determines the simulation method to obtain the surface tension. As examples, methods based on the finite-size scaling approach developed by Binder²⁴ are useful to model the critical region,²⁵ while area-perturbation based methods are difficult to implement in that region due to the stabilization of the liquid slab.²⁶ In the finite-size formalism, the surface tension is obtained for an infinite system size; finite size effects have been observed in other methods for simulations boxes with small cross sectional areas, $A = L_x \times L_y < (10\sigma)^2$, being σ the molecular diameter. An oscillatory behavior for surface tension that decays with the surface area of the interface, has been reported for Lennard-Jones and square-well systems. This effect could be

^{a)}Electronic mail: gil@fisica.ugto.mx.

present even in bulk systems for non-cubic simulation boxes, resulting in a non-isotropic pressure tensor.^{25–30}

Also, some problems have been identified in VP and TA methods, when applying forward and reverse perturbations for systems with discontinuous potentials.^{9,11,12,15,26} In this article we present a methodology to apply the VP method for non-spherical systems interacting via discontinuous potentials, extending previous results found by Jackson and co-workers,^{14,15} and trying to obtain a criteria to select the simulation parameters. The theoretical framework is developed in Sec. II, where a general expression to calculate the pressure for the systems of interest is given. Details of Monte Carlo simulations performed for several systems in order to test our approach are given in Sec. III, and results are presented in Sec. IV. Conclusions are given in Sec. V.

II. METHOD

A general methodology will be described now, implemented for the computer simulation of several systems with discontinuous potentials:

- (A) For the sake of simplicity, we will show through the virial route that for a discontinuous potential the pressure can be written as a sum of terms related to each discontinuity. As virial and thermodynamic expressions for pressure are formally equivalent,⁵ this additivity feature is also valid for the pressure calculated from the thermodynamic route. We will detail the case of the square-well potential, where the pressure will have an ideal contribution and two excess terms, one from each discontinuity: at the hard-body (HB) distance and at the square-well (SW) width.
- (B) We will use the results from Brumby *et al.*¹⁵ for hard-body non-convex molecules, and identify this as the contribution to the pressure from the HB discontinuity.
- (C) In analogy to the cited methodology, we will obtain the contribution to the pressure from the SW width discontinuity.
- (D) Then, a final expression for the pressure is given in a more practical way, using some identities that were found in the simulation tests.
- (E) From the previous results we will infer the generalization to m -discontinuities.
- (F) Finally, we give the expression for the surface tension, which will be used to test our methodology.

A. Additivity in pressure for discontinuous potentials

The mechanical method based on the Clausius virial theorem^{1,2} allow us to evaluate the pressure in a molecular simulation. Assuming a system with pairwise interactions in the absence of external fields, the usual virial form for pressure is

$$p = \langle \rho k_B T \rangle + \left\langle \frac{1}{3V} \sum_i \sum_{i < j} \mathbf{r}_{ij} \cdot \mathbf{f}_{ij} \right\rangle, \quad (1)$$

where the angular brackets indicate the statistical average in the appropriate ensemble, $\rho = N/V$ is the number density, k_B is the Boltzmann constant, T is the temperature, \mathbf{r}_{ij} is the intermolecular vector between a molecular pair, and \mathbf{f}_{ij} is the corresponding intermolecular force.

For a central potential $u(r)$, Eq. (1) can be written in terms of the distribution function $g(r)$, as

$$\begin{aligned} \frac{\beta p}{\rho} &= 1 - \frac{2\pi\beta\rho}{3} \int r^3 \frac{du(r)}{dr} g(r) dr \\ &= 1 + \frac{2\pi\rho}{3} \int r^3 \frac{de^{-\beta u(r)}}{dr} y(r) dr, \end{aligned} \quad (2)$$

where we have used the cavity function $y(r) = g(r)e^{\beta u(r)}$ and $\beta = 1/k_B T$. In the case of potentials with m discontinuities,

$$u(r) = \begin{cases} \epsilon_1 & \text{if } 0 \leq r \leq \lambda_1\sigma \\ \epsilon_2 & \text{if } \lambda_1\sigma < r \leq \lambda_2\sigma \\ \vdots & \\ \epsilon_m & \text{if } \lambda_{m-1}\sigma < r \leq \lambda_m\sigma \\ 0 & \text{if } r > \lambda_m\sigma \end{cases}, \quad (3)$$

where σ is the hard-spheres diameter.

For this potential, we can write

$$\frac{de^{-\beta u(r)}}{dr} = \sum_{\alpha=1}^m C_\alpha \delta(r - \lambda_\alpha\sigma), \quad (4)$$

that can be substituted in Eq. (2),

$$\frac{\beta p}{\rho} = 1 + \frac{2\pi\rho}{3} \sum_{\alpha} C_\alpha (\lambda_\alpha\sigma)^3 y(\lambda_\alpha\sigma). \quad (5)$$

The coefficients C_α can be obtained by integrating Eq. (4) in the vicinity of each discontinuity,

$$C_\alpha = \int_{\lambda_\alpha\sigma^-}^{\lambda_\alpha\sigma^+} \frac{de^{-\beta u(r)}}{dr} dr = e^{-\beta u(\lambda_\alpha\sigma^+)} - e^{-\beta u(\lambda_\alpha\sigma^-)}, \quad (6)$$

where the + and – signs indicate the evaluation of the function's discontinuity from the right and left sides, respectively. Since the cavity function is continuous, then the following relation holds

$$C_\alpha y(\lambda_\alpha\sigma) = g(\lambda_\alpha\sigma^+) - g(\lambda_\alpha\sigma^-), \quad (7)$$

and Eq. (5) can be written as

$$\begin{aligned} p &= \frac{Nk_B T}{V} + \frac{2\pi k_B T}{3} \left(\frac{N}{V}\right)^2 \sum_{\alpha} (\lambda_\alpha\sigma)^3 \\ &\quad \times [g(\lambda_\alpha\sigma^+) - g(\lambda_\alpha\sigma^-)] \\ &= p_{ideal} + p_{excess} \\ &= p_{ideal} + p_{exc}^{(1)} + p_{exc}^{(2)} + \cdots + p_{exc}^{(m)}, \end{aligned} \quad (8)$$

where we have identified an ideal and excess contribution to pressure and, in the last line, we have labeled each excess contribution term as the discontinuity to which is related.

Up to here, for the sake of simplicity, we have used the virial expression for the pressure, to show the relation between the additivity in pressure and the potential discontinuities. However, we are interested in the thermodynamic route,

since it is easier to implement in Monte Carlo simulations at constant volume for discontinuous systems. Taking advantage of the equivalence between both routes,⁵ we will take the additivity feature of Eq. (8) for the second case, in order to evaluate the pressure using the volume perturbation method.

Now, we will focus on a discontinuous potential of the form of a square-well interaction,

$$u(d) = \begin{cases} \infty & \text{if } 0 \leq d \leq \sigma \\ \epsilon & \text{if } \sigma < d \leq \lambda\sigma, \\ 0 & \text{if } d > \lambda\sigma \end{cases}, \quad (9)$$

where d denotes the atom-atom distance for simple fluids, site-site distance for chain molecules, or minimal distance for convex geometries, such as spherocylinders. It is necessary to decompose the pair potential into its repulsive and attractive contributions; we selected the Weeks-Chandler-Andersen criteria,³¹ $u(d) = u_{HB}(d) + u_{SW}(d)$, where

$$u_{HB}(d) = \begin{cases} \infty & \text{if } d \leq \sigma \\ 0 & \text{if } d > \sigma, \end{cases} \quad (10)$$

$$u_{SW}(d) = \begin{cases} \epsilon & \text{if } d \leq \lambda\sigma \\ 0 & \text{if } d > \lambda\sigma. \end{cases} \quad (11)$$

The corresponding expression for the pressure is given by

$$p = p_{ideal} + p_{exc}^{(HB)} + p_{exc}^{(SW)}. \quad (12)$$

B. Hard-body discontinuity contribution

The HB term was calculated by Brumby *et al.*,¹⁵ showing that for non-spherical particles, increments of volume of the simulation cell could cause overlaps. These overlaps produce a contribution to the pressure that was not considered before.⁹ For an isothermal-isobaric ensemble (NPT), the enthalpy changes arising from variation in the volume are related to the transition probability between states, and the detailed balance condition implies that

$$\left\langle \exp\left(-\frac{\Delta U_{i \rightarrow j-}}{k_B T}\right) \right\rangle_{eq} = \exp\left(-\frac{p \Delta V_{i \rightarrow j+}}{k_B T}\right) \times \left\langle \exp\left(-\frac{\Delta U_{i \rightarrow j+} - N k_B T \ln[1 + (\Delta V_{i \rightarrow j+}/V_i)]}{k_B T}\right) \right\rangle_{eq}, \quad (13)$$

where i denotes the initial state at volume V_i , j the final state after a volume change ΔV , ΔU the energy change, and the subscripts $+$ and $-$ indicate if the volume change is positive (expansion) or negative (compression).

The previous equation is valid for simulations in the canonical ensemble (NVT) if volume changes are treated as virtual perturbations, and the following expression for $p^{(HB)}$

can be obtained,

$$p^{(HB)} = \frac{N k_B T}{V_i} + \lim_{\Delta V_{i \rightarrow j+} \rightarrow 0} \frac{k_B T}{\Delta V_{i \rightarrow j+}} \ln \left\langle \exp\left(-\frac{\Delta U_{i \rightarrow j+}^{(HB)}}{k_B T}\right) \right\rangle_{eq} + \lim_{\Delta V_{i \rightarrow j-} \rightarrow 0} \frac{k_B T}{\Delta V_{i \rightarrow j-}} \ln \left\langle \exp\left(-\frac{\Delta U_{i \rightarrow j-}^{(HB)}}{k_B T}\right) \right\rangle_{eq}, \quad (14)$$

where we have labeled the pressure and energy as HB, i.e., the hard-body contribution. Using the same notation as in Eq. (12) we can express $p_{exc}^{(HB)}$ as the sum of compression and expansion contributions,

$$p_{exc}^{(HB)} = p_+^{(HB)} + p_-^{(HB)}, \quad (15)$$

where

$$p_+^{(HB)} = \lim_{\Delta V_{i \rightarrow j+} \rightarrow 0} \frac{k_B T}{\Delta V_{i \rightarrow j+}} \ln \left\langle \exp\left(-\frac{\Delta U_{i \rightarrow j+}^{(HB)}}{k_B T}\right) \right\rangle_{eq}, \quad (16)$$

and an analogous expression states for the compression contribution $p_-^{(HB)}$.

C. Square-well discontinuity contribution

Following Brumby *et al.*,¹⁵ we will consider now the attractive contribution to the pressure. The transition probability from state i to state j , $P_{i \rightarrow j}$ in a Monte Carlo computer simulation in the isothermal-isobaric ensemble, for an infinitesimal volume change $\Delta V_{i \rightarrow j} = V_j - V_i$, is given by

$$P_{i \rightarrow j} = \exp\left(-\frac{\Delta H_{i \rightarrow j}}{k_B T}\right), \quad (17)$$

where $\Delta H_{i \rightarrow j}$ is the enthalpy change,

$$\Delta H_{i \rightarrow j} = \Delta U_{i \rightarrow j} + p \Delta V_{i \rightarrow j} - N k_B T \ln\left(\frac{V_j}{V_i}\right). \quad (18)$$

At equilibrium, the detailed balance condition for random changes in the volume is given by

$$\sum_{n^+} \Delta V_{i \rightarrow j+} P_{i \rightarrow j+} = - \sum_{n^-} \Delta V_{i \rightarrow j-} P_{i \rightarrow j-}, \quad (19)$$

where n^+ and n^- are the number of volume changes for expansion and compression, respectively. Since for an infinite number of volume changes $n^+ = n^-$, then

$$\langle \Delta V_{i \rightarrow j+} P_{i \rightarrow j+} \rangle_{eq} = - \langle \Delta V_{i \rightarrow j-} P_{i \rightarrow j-} \rangle_{eq}. \quad (20)$$

Assuming infinitesimal volume changes, $\Delta V_{i \rightarrow j}/V_i$ is small, then $\ln[1 + (\Delta V_{i \rightarrow j}/V_i)] \approx \Delta V_{i \rightarrow j}/V_i$, and Eq. (18) transforms into the following expression:

$$\Delta H_{i \rightarrow j} = \Delta U_{i \rightarrow j} + \Delta V_{i \rightarrow j} \left(p - \frac{N k_B T}{V_i} \right). \quad (21)$$

If we consider the attractive potential given by Eq. (11), i.e., we do not take into account overlaps due to a hard-body restriction, then we need to derive expressions for enthalpy changes for compression and expansions.

Considering an expansion, $\Delta V_{i \rightarrow j+} > 0$, the change on enthalpy is given by

$$\Delta H_{i \rightarrow j+} = \Delta U_{i \rightarrow j+} + \Delta V_{i \rightarrow j+} \left(p - \frac{Nk_B T}{V_i} \right). \quad (22)$$

The sign on the second term depends on the relation between p and the ideal pressure. For a SW system we know that such quantity could be positive or negative depending on the thermodynamic conditions, and we cannot say anything *a priori* about the sign of $\Delta H_{i \rightarrow j+}$, an important difference with respect to repulsive HB interactions. The transition probability is given by

$$P_{i \rightarrow j+} = \exp \left[-\frac{\Delta U_{i \rightarrow j+} + \Delta V_{i \rightarrow j+} \left(p - \frac{Nk_B T}{V_i} \right)}{k_B T} \right]. \quad (23)$$

For the case of a compression, i.e., $\Delta V_{i \rightarrow j-} < 0$, the change on enthalpy is

$$\Delta H_{i \rightarrow j-} = \Delta U_{i \rightarrow j-} + \Delta V_{i \rightarrow j-} \left(p - \frac{Nk_B T}{V_i} \right). \quad (24)$$

The second term in this equation has a negative contribution from the $\Delta V_{i \rightarrow j-}$ factor, but the difference between p and the ideal pressure can be positive or negative. Then, we cannot say anything *a priori* about the sign of $\Delta H_{i \rightarrow j-}$. The transition probability is given by

$$P_{i \rightarrow j-} = \exp \left[-\frac{\Delta U_{i \rightarrow j-} + \Delta V_{i \rightarrow j-} \left(p - \frac{Nk_B T}{V_i} \right)}{k_B T} \right]. \quad (25)$$

Using in Eq. (20) both expressions for the transition probabilities, Eqs. (23) and (25), we obtain

$$\begin{aligned} & \left\langle \Delta V_{i \rightarrow j+} \exp \left[-\frac{\Delta U_{i \rightarrow j+} + \Delta V_{i \rightarrow j+} \left(p - \frac{Nk_B T}{V_i} \right)}{k_B T} \right] \right\rangle_{eq} \\ &= - \left\langle \Delta V_{i \rightarrow j-} \exp \left[-\frac{\Delta U_{i \rightarrow j-} + \Delta V_{i \rightarrow j-} \left(p - \frac{Nk_B T}{V_i} \right)}{k_B T} \right] \right\rangle_{eq}, \end{aligned} \quad (26)$$

Considering that volume changes are constant, i.e., $\Delta V_{i \rightarrow j+} = -\Delta V_{i \rightarrow j-}$, then

$$\begin{aligned} & \exp \left(-\frac{p \Delta V_{i \rightarrow j+}}{k_B T} \right) \left\langle \exp \left(\frac{N \Delta V_{i \rightarrow j+}}{V_i} \right) \exp \left(-\frac{\Delta U_{i \rightarrow j+}}{k_B T} \right) \right\rangle_{eq} \\ &= \exp \left(\frac{p \Delta V_{i \rightarrow j+}}{k_B T} \right) \left\langle \exp \left(-\frac{N \Delta V_{i \rightarrow j+}}{V_i} \right) \right. \\ & \quad \times \left. \exp \left(-\frac{\Delta U_{i \rightarrow j-}}{k_B T} \right) \right\rangle_{eq}, \end{aligned} \quad (27)$$

and we can solve for the pressure by taking logarithms at both sides of this equation,

$$\begin{aligned} \frac{2p \Delta V_{i \rightarrow j+}}{k_B T} &= - \ln \left\langle \exp \left(\frac{N \Delta V_{i \rightarrow j+}}{V_i} \right) \exp \left(-\frac{\Delta U_{i \rightarrow j+}}{k_B T} \right) \right\rangle_{eq} \\ &+ \ln \left\langle \exp \left(-\frac{N \Delta V_{i \rightarrow j+}}{V_i} \right) \exp \left(-\frac{\Delta U_{i \rightarrow j-}}{k_B T} \right) \right\rangle_{eq}. \end{aligned} \quad (28)$$

This expression is valid for infinitesimal volume changes in the NPT ensemble, but in analogy to the HB contribution calculation,¹⁵ we will use this result to obtain the pressure in a NVT ensemble, using a volume perturbation method. In the NVT ensemble, V_i is constant so the infinitesimal volume change corresponds to a virtual perturbation that is not included in the Markov simulation chain, and Eq. (28) can be rewritten as

$$\begin{aligned} -\frac{2p \Delta V_{i \rightarrow j+}}{k_B T} &= -\frac{2N \Delta V_{i \rightarrow j+}}{V_i} - \ln \left\langle \exp \left(-\frac{\Delta U_{i \rightarrow j+}}{k_B T} \right) \right\rangle_{eq} \\ &+ \ln \left\langle \exp \left(-\frac{\Delta U_{i \rightarrow j-}}{k_B T} \right) \right\rangle_{eq}. \end{aligned} \quad (29)$$

Multiplying both sides by $-k_B T / 2 \Delta V_{i \rightarrow j+}$, remembering that this is valid in the limit $\Delta V_{i \rightarrow j+} \rightarrow 0$, and using $\Delta V_{i \rightarrow j+} = -\Delta V_{i \rightarrow j-}$, a symmetric expression for the pressure is obtained

$$\begin{aligned} p^{(SW)} &= \frac{Nk_B T}{V_i} + \frac{1}{2} \lim_{\Delta V_{i \rightarrow j+} \rightarrow 0} \frac{k_B T}{\Delta V_{i \rightarrow j+}} \ln \left\langle \exp \left(-\frac{\Delta U_{i \rightarrow j+}^{(SW)}}{k_B T} \right) \right\rangle_{eq} \\ &+ \frac{1}{2} \lim_{\Delta V_{i \rightarrow j-} \rightarrow 0} \frac{k_B T}{\Delta V_{i \rightarrow j-}} \ln \left\langle \exp \left(-\frac{\Delta U_{i \rightarrow j-}^{(SW)}}{k_B T} \right) \right\rangle_{eq}, \end{aligned} \quad (30)$$

where, in analogy to Eq. (14), we have labeled the pressure and energy by a superscript SW, i.e., the attractive contribution to the potential. In Eq. (30) we can identify the excess pressure contributions arising from expansions and compressions,

$$p_{exc}^{(SW)} = \frac{1}{2} [p_+^{(SW)} + p_-^{(SW)}], \quad (31)$$

where

$$p_+^{(SW)} = \lim_{\Delta V_{i \rightarrow j+} \rightarrow 0} \frac{k_B T}{\Delta V_{i \rightarrow j+}} \ln \left\langle \exp \left(-\frac{\Delta U_{i \rightarrow j+}^{(SW)}}{k_B T} \right) \right\rangle_{eq}, \quad (32)$$

and an equivalent expression holds for the compression contribution $p_-^{(SW)}$.

D. HB + SW pressure and some identities

We can now obtain the expression for the total pressure considering the hard-body and square-well contributions derived previously. By substituting Eqs. (15) and (31) in Eq. (12), we obtain

$$p = p_{ideal} + p_+^{(HB)} + p_-^{(HB)} + \frac{1}{2} [p_+^{(SW)} + p_-^{(SW)}]. \quad (33)$$

As we report in Sec. IV, from the computer simulations performed in our study we also found that,

$$p_+^{(SW)} = p_-^{(SW)}, \quad (34)$$

$$p_-^{(HB+SW)} = p_-^{(HB)} + p_-^{(SW)}, \quad (35)$$

where the label HB + SW indicates that both interactions are taken into account at the same time. The first relation can be understood due to the symmetry between two events: those particles that cross the potential discontinuity in one direction when the volume is increased, and those that cross in the opposite direction when volume decreases. So the magnitude of the changes in energy in one and another cases should be the same. Applying the exponential function (see Eq. (32)), its ensemble average and then the logarithm function, should give very similar numbers but with opposite sign. This sign is canceled by the factor $\Delta V_{i \rightarrow j}$ that is opposite in each case. This symmetry does not appear in the HB discontinuity, since overlaps in expansions are less likely to happen.

The second relation can be seen as a particular case of the additivity properties of the pressure. The contribution to pressure, given by a test volume compression in the case of a square-well system, should be the sum of the contribution from the HB and the attractive SW discontinuities calculated from compressions.

These relations allow us to reformulate the expression for the total pressure. Substitution of relations (34) and (35) in Eq. (33) gives

$$p = p_{ideal} + p_-^{(HB+SW)} + p_+^{(HB)}, \quad (36)$$

which is a more practical expression from the point of view of a computer simulation calculation. The second term means that for compressions the complete potential contributes, while for expansions only the HB contribution should be taken into account. An alternative form of Eq. (36) is

$$p = p_{ideal} + p_-^{(HB)} + p_+^{(HB+SW)}, \quad (37)$$

which is obtained from Eq. (33) using the relation (34) and the expansion version of relation (35): $p_+^{(HB+SW)} = p_+^{(HB)} + p_+^{(SW)}$.

To evaluate the components of the pressure tensor using the test volume method, an anisotropic virtual change in volume is required. If the component is p_{xx} , the length of the simulation box changes from L_x, L_y, L_z to $L_x + \Delta L_x, L_y, L_z$. We can define a volume perturbation parameter given by

$$\xi = \Delta V/V, \quad (38)$$

i.e., for the case considered here, the length of the x axis is increased by a factor $(1 + \xi)$ while the other two sides are kept constant. For this particular case, $\xi = \Delta L_x/L_x$.

E. Generalization to m discontinuities

For a discontinuous potential with m discontinuities (where $m = 1$ corresponds to the HB repulsion), we can extend the result obtained for a SW fluid in Eq. (36), and then

the pressure is

$$p^{(m)} = p_{ideal} + p_-^{(HB,m)} + p_+^{(HB)}, \quad (39)$$

where $p_-^{(HB,m)}$ is now the pressure contribution from compression taking into account all the potential discontinuities. This equation is obtained by assuming the generalization of Eqs. (34) and (35), since the same arguments used for the SW potential are valid for arbitrary attractive or repulsive discontinuities. Eppenga and Frenkel⁹ suggested that for a hard-body fluid only compressions must be taken into account. However, as demonstrated by Brumby *et al.*,¹⁵ for non-spherical molecules there is an unexpected contribution coming from overlaps when the volume of the system is increased, and Eq. (39) is consistent with this result.

F. Surface tension

The volume perturbation method can be applied performing anisotropic volume changes in order to calculate the pressure tensor, p_{ij} , where $i, j = x, y, z$. For a fluid in hydrostatic conditions, all the non-diagonal elements are null and the pressure p is given by one third of the trace of p_{ij} , i.e., $p = (p_{xx} + p_{yy} + p_{zz})/3$. The pressure tensor also can be used to calculate the surface tension γ for systems with interfaces.

Assuming a planar interface lying in the x - y plane, the components of the pressure tensor depend on the distance z to the interface,^{1,3}

$$\gamma = \int_{-\infty}^{\infty} dz [p_N(z) - p_T(z)], \quad (40)$$

where $p_N(z)$ is the local pressure normal to the surface, $p_N(z) = p_{zz}(z)$ in our case, and $p_T(z)$ is the local pressure tangential to the surface, defined by $p_T(z) = (p_{xx}(z) + p_{yy}(z))/2$. Since we are considering an interface that is isotropic in the x and y directions, then $p_{xx}(z) = p_{yy}(z)$. For planar interfaces, the mean-value theorem allows to write the last expression in terms of the macroscopic normal and tangential components, P_N and P_T ,^{13,15,22}

$$\gamma = \frac{1}{2} L_z [P_N - P_T], \quad (41)$$

where the factor 2 takes into account the two interfaces of the simulated system.

III. MONTE CARLO SIMULATIONS

We applied the virtual volume perturbation method to several systems in MC-NVT simulations (MC-NVT + VP). Results are given for: (a) tests of the method for flexible SW chain molecules, (b) extension to other flexible discrete-potentials chain molecules and spherocylinders, and (c) calculation of the surface tension. Variables are reported in reduced units: temperature $T^* = k_B T/\epsilon$, density $\rho^* = \rho \sigma^3 = (N/V)\sigma^3$ being N the number of molecules, pressure $P^* = p\sigma^3/k_B T$, and surface tension $\gamma^* = \gamma\sigma^2/k_B T$. According to these reduced variables, the ideal contribution to pressure is given by $p_{ideal}^* = \rho^*$. The simulation cell dimensions are scaled as $L_i^* = L_i/L_x$ for $i = x, y, z$.

A. Tests for flexible SW chain molecules

The first group of simulations was used to test the volume perturbation method as a tool to calculate the pressure tensor for a discontinuous-potential primitive model, a 3-mer SW flexible molecule. This model allows us to test the method with non-convex molecules with internal flexibility, which we consider very general. SW chain-like models are interesting since they can model polymers and surfactant molecules. SW parameters are the hard-spheres diameter σ , the attractive range $\lambda = 1.5\sigma$ and the energy depth $\epsilon = -1.0$; intramolecular attractions account for monomers separated for more than one junction.

Two simulation boxes were used to check the independence of the method respect to the cell shape. The first, labeled as “Box 1,” is a cubic cell, $L_x^* = L_y^* = L_z^*$, while the second, labeled as “Box 2,” is an elongated cell with $L_x^* \times L_y^* \times L_z^* = 1 \times 1 \times 8$. The cell contains $N = 1024$ particles at temperature $T^* = 2.5$, which is supercritical.³² A series of Monte Carlo simulations in the isothermal-isobaric ensemble (MC-NPT) were performed with a fcc lattice as initial configuration. Every molecule movement is comprised of a displacement, rigid body rotation and internal torsion, chosen in a random way. A complete cycle is given by one movement per particle on average and a volume change; around $1-2 \times 10^6$ cycles were required for equilibration and a similar number of cycles were used for averaging. For a fixed P^* , the equilibrium density was obtained and the output configuration was used as the input for the next state at a higher pressure. These simulations give the density for a specified value of the pressure, information that is useful in order to test the volume perturbation-method runs.

Some states from the MC-NPT simulations were selected and the average density in equilibrium, ρ^* , was used as an input for MC-NVT simulations. First, a short simulation (5×10^5 cycles) was carried out to disorder the fcc initial configuration for a purely hard system. Using the final configuration, we switched-on the SW potential and performed a MC-NVT simulation of 10^6 cycles to equilibrate. Finally, with an equilibrated system, the MC-NVT + VP simulation was performed in order to obtain the diagonal pressure components, p_{xx}^* , p_{yy}^* , and p_{zz}^* . One configuration every cycle was taken to apply the virtual volume change and $3-5 \times 10^6$ cycles were used for these averages.

B. Other systems

To apply the method to other molecular models and different discontinuous potentials, two systems were studied. The first one is a system of hard spherocylinders with an additional attractive contribution (SWSC) with aspect ratio $L^* = L/\sigma$, where L is the length of the hard cylinder and σ is the diameter of the hemispherical hard caps. With this model we study the performance of the VP method with convex molecules, and since spherocylinders are a basic primitive model to study liquid crystalline phases, this system allows us to test the VP method in orientational and positional ordered systems.

Particles interact via a SWSC potential defined by

$$u_{swsc}(d) = \begin{cases} \infty & \text{if } d(r, \Omega) \leq \sigma \\ -1 & \text{if } \sigma \leq d(r, \Omega) < 1.5\sigma \\ 0 & \text{if } d(r, \Omega) > 1.5\sigma \end{cases}, \quad (42)$$

where $d(r, \Omega)$ is the minimum distance between the molecular axis of a pair of particles whose centers are separated by a distance r for a relative orientation Ω .³³⁻³⁵ A cubic simulation cell was used with $N = 1020$ particles and temperature $T^* = 5.0$.

The second system also was a 3-mer flexible chain, where now monomers interact via a hard sphere plus a combination of repulsive shoulder and attractive square-well (SS + SW) potentials:

$$u(r) = \begin{cases} \infty & \text{if } 0 \leq r \leq \sigma \\ 0.5 & \text{if } \sigma < r \leq 1.4\sigma \\ -1.0 & \text{if } 1.4\sigma < r \leq 1.7\sigma \\ 0 & \text{if } r > 1.7\sigma \end{cases}, \quad (43)$$

where r is the site-site distance. This model allows to verify our generalization to potentials with several discontinuities. The simulation cell for this system was a cubic box with $N = 1024$ chains and temperature $T^* = 3.0$.

For both systems, MC-NPT simulations were carried out with $\sim 2 \times 10^6$ cycles to equilibrate and $1-2 \times 10^6$ cycles to average properties. For a fixed P^* , the equilibrium density was obtained and the output configuration was used as the input for the next state at a higher pressure. These simulations give the density for a specified value of the pressure, information that is useful in order to test the volume perturbation-method runs.

The resulting density of some states was used as the fixed value to perform MC-NVT simulations. First, to disorder the initial fcc lattice configuration, a short simulation (5×10^5 cycles) was performed for a purely HB system. Then, using the respective potential for each system at the temperatures of interest, equilibration simulations were performed with $1-3 \times 10^6$ cycles. In the case of nematic and smectic phases for the SWSC system, the order parameters were in concordance with the MC-NPT averages. Finally, having equilibrated configurations, the MC-NVT + VP simulations were obtained with 8×10^6 cycles. The virtual volume change was implemented each 10 cycles and 4 groups of independent simulations were averaged for each state, in order to improve the statistics.

C. Surface tension

Surface tension values were obtained for the flexible 3-mer SW chain molecules with the same model parameters given in Sec. III A. Direct coexistence simulations were performed in an elongated simulation cell “Box 2,” with dimensions $L_x^* \times L_y^* \times L_z^* = 1 \times 1 \times 8$, with $L_x \sim 12\sigma$, and using $N = 1152$ particles. This cell has a cross sectional area greater than $(10\sigma)^2$ to avoid size-system effects, following previous studies by several authors.^{25,26,28-30}

The initial configuration consisted of an array of compact slabs of molecules, where particles in every slab are arranged

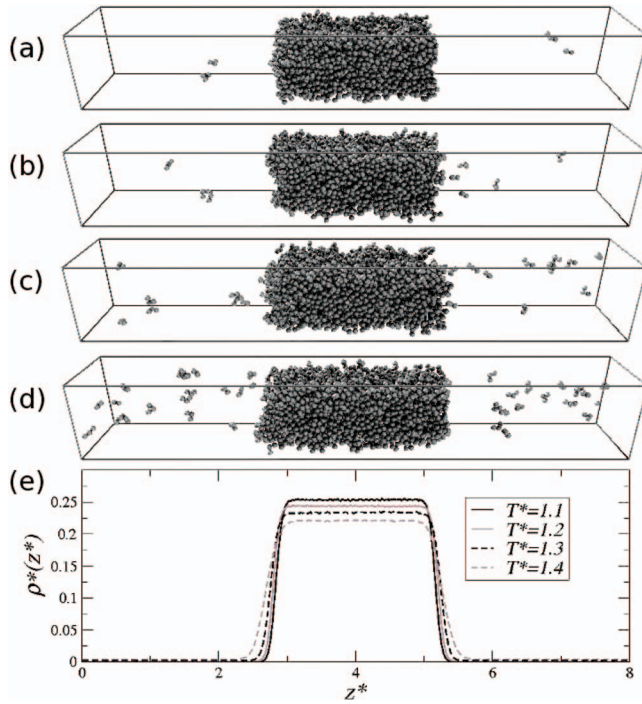


FIG. 1. (a)–(d) Equilibrated configurations for MC-NVT + VP simulations. The system consisted of 3-mer SW chains in the simulation cell “Box 2” using 1152 molecules. The fixed density was $\rho^* = 0.0738$ and each snapshot corresponds to temperatures $T^* = 1.1$, $T^* = 1.2$, $T^* = 1.3$, and $T^* = 1.4$. (e) Density profile as a function of the major axis of the simulation cell in reduced units, $z^* = z/L_x$. For each monomer, the density profile was calculated from simulation, averaging over equilibrium configurations. The profiles given in the graphic correspond to the average over the three monomers profiles. The states are the same as those in (a)–(d).

as in a simple cubic lattice. The slabs were centered respect to the long z side of the box, so that free space was left at both sides of the initial array. MC-NVT simulations were performed with a fixed density $\rho^* = 0.0738$ and at a subcritical temperature $T^* = 1.3$,³² obtaining a liquid slab located in the middle of a large simulation box. The reported density does not correspond to the density within the liquid slab but rather the overall density of the system including the large vapor region surrounding the liquid slab. Around 2×10^6 cycles were required for equilibration and the output was used to simulate higher and lower temperatures, Figs. 1(a)–1(d). The equilibrated states were used to run MC-NVT + VP simulations with a virtual volume change every cycle. The averages for the pressure were calculated over 8 groups of independent simulations, performing a virtual volume change every cycle and using 8×10^6 cycles for each simulation.

The normal component to the interface of the pressure tensor, p_{zz}^* , should correspond to the vapor pressure of the system. To evaluate this, we obtained the vapor density ρ_V^* from the density profile, which was calculated from the average of configurations for each state. Then, independent MC-NPT simulations at very low pressure were performed in a cubic box for $N = 256$ molecules, in order to obtain average density values ρ^* for each pressure P^* . From a linear fit of these data, a relation between the ρ_V^* and its corresponding vapor pressure, p_V^* , was obtained.

TABLE I. Pressure tensor, $p_{\alpha\alpha}^* = p_{\alpha\alpha}\sigma^3/k_B T$ with $\alpha = x, y, z$, calculated by MC-NVT + VP simulations for different values of the volume perturbation parameter $|\xi| = |\Delta V|/V$. Results are given for a system of $N = 1024$ 3-mer SW chains, at a density of $\rho^* = 0.2215$ and at a supercritical temperature $T^* = 2.5$. The pressure corresponding to this state is $P^* = 1.0$, according to MC-NPT simulations. VP method was applied, using Eq. (36), to configurations taken every cycle and results correspond to averages over $3\text{--}5 \times 10^6$ configurations. Two simulation cells with different shape were used, labeled as “Box 1” and “Box 2.”

$ \xi $	Simulation box	p_{xx}^*	p_{yy}^*	p_{zz}^*	No overlap (%)
0.00001	Box 1	0.98(3)	1.01(1)	0.98(3)	91
	Box 2	0.99(3)	1.00(3)	1.00(3)	91
0.00005	Box 1	0.993(8)	0.993(9)	1.00(1)	62
	Box 2	0.993(6)	0.995(6)	0.988(5)	62
0.00010	Box 1	0.997(8)	0.993(5)	0.997(6)	39
	Box 2	0.997(6)	0.994(7)	0.989(7)	39
0.00020	Box 1	0.998(7)	0.996(5)	0.996(5)	15
	Box 2	0.996(7)	0.998(4)	0.99(1)	15
0.00030	Box 1	0.995(9)	0.995(3)	0.994(4)	6
	Box 2	0.993(6)	1.001(4)	1.00(1)	6
0.00040	Box 1	1.00(1)	0.997(5)	1.006(5)	2
	Box 2	0.996(8)	1.00(1)	0.993(8)	2

The density profiles for each studied temperature are shown in Figure 1(e), as functions of the long axis of the box in reduced units, $z^* = z/L_x$.

IV. RESULTS AND DISCUSSION

A. Tests for flexible SW chain molecules

Formally, the limits of Eqs. (14) and (30) imply that the thermodynamic pressure P^* can be obtained by considering pressures for several values of the volume perturbation parameter, $|\xi| = |\Delta V|/V$, in order to extrapolate P^* when $|\xi| \rightarrow 0$. For the case of continuous potentials P^* has a linear behavior respect to $|\xi|$. For such cases, de Miguel and Jackson¹³ have shown that the pressure calculated from compression ($\xi < 0$) is symmetric to the pressure calculated from expansion ($\xi > 0$), both given as functions of $|\xi|$. The actual value of P^* is given by the limit $|\xi| \rightarrow 0$ or from the arithmetic average of the pressure values at compression and expansion for a single value of $|\xi|$.

For discontinuous potential systems the situation is more complex and is not possible to follow the extrapolation procedure. In Table I we present the pressure tensor calculated from Eq. (36) for several values of $|\xi|$, the equivalence between Eqs. (33) and (36) will be shown later. A third of the trace of the pressure tensor, $P^* = (p_{xx}^* + p_{yy}^* + p_{zz}^*)/3$ is given in Fig. 2(a) as a function of $|\xi|$. Similar results for each contribution are sketched in Fig. 2(b) for compression, $p_{-}^{*(HB+SW)}$, and in Fig. 2(c) for expansion, $p_{+}^{*(HB)}$. Taking into account that the slope of the results presented in Fig. 2 is quite small (in fact is almost a horizontal line) and considering that the statistical uncertainty increases considerably for small values of $|\xi|$, it seems reasonable to take a single value of $|\xi|$ to estimate P^* if a criterion is found for doing this.

In Fig. 3 we present the simulated pressure for different values of $|\xi|$ and as a function of the number of test volume

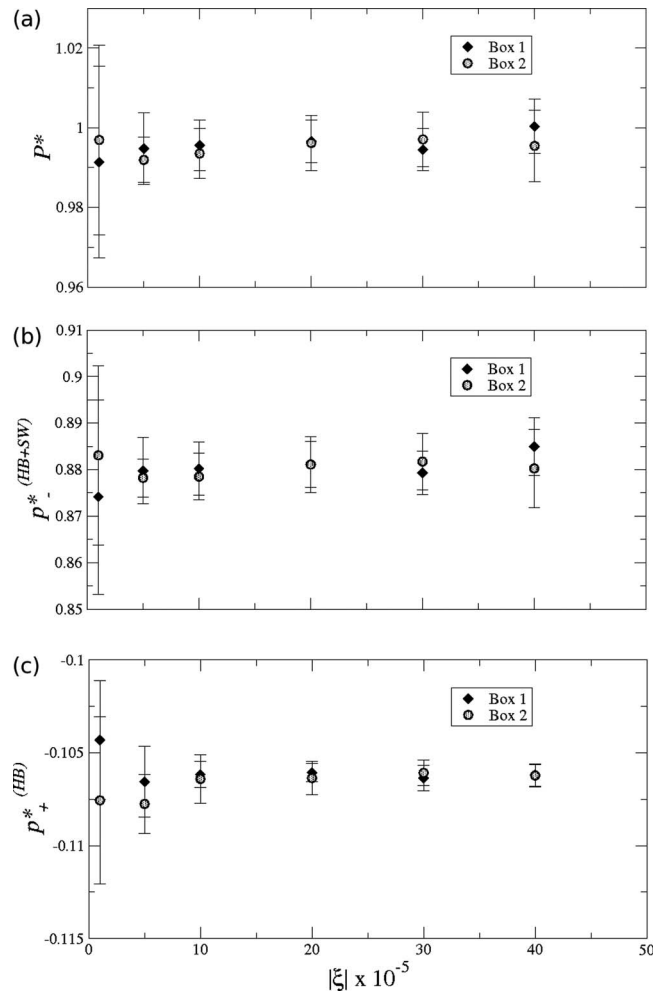


FIG. 2. Pressure, $P^* = \rho\sigma^3/k_B T$, as a function of the volume perturbation value $|\xi| = |\Delta V|/V$. Graphics correspond to: (a) complete pressure P^* , calculated from Eq. (36); (b) compression contribution to pressure $p_{-(HB+SW)}^*$, calculated for the total potential HB+SW; (c) expansion contribution to pressure $p_{+(HB)}^*$, which takes into account only HB interactions. Simulations were carried out with $N = 1024$ 3-mer SW chains, at a density $\rho^* = 0.2215$ and at a supercritical temperature $T^* = 2.5$. The pressure corresponding to this state is $P^* = 1.0$, according to MC-NPT simulations. The volume perturbation was applied to configurations taken every cycle and results correspond to averages over $3\text{--}5 \times 10^6$ configurations. In all the cases, pressure tensor components were calculated directly from the simulation, and the pressure is given by $P^* = (p_{xx}^* + p_{yy}^* + p_{zz}^*)/3$. Two simulation cells with different shape were used, labeled as “Box 1” and “Box 2.”

trials. We considered $|\xi| = 1 \times 10^{-5}$, 20×10^{-5} , and 40×10^{-5} . In the simulation, smaller values of $|\xi|$ imply lower percentage of HB overlapping configurations when compressing; then small $|\xi|$ values are not adequate to determine the pressure. For the system studied here, a compression with $|\xi| = 1 \times 10^{-5}$ generates 2% of HB overlapping configurations in a 3×10^6 sample (see also Table I). This case is presented as the curve with more noisy behavior in Fig. 3; it is also the most dissimilar case between Boxes 1 and 2, as seen in Fig. 2. For larger $|\xi|$ values these effects are less noticeable. The results given in Fig. 3 are the worst correspondence between curves in the studied cases.

For an adequate selection of $|\xi|$ we propose to check the percentage of HB overlapping configurations for several $|\xi|$

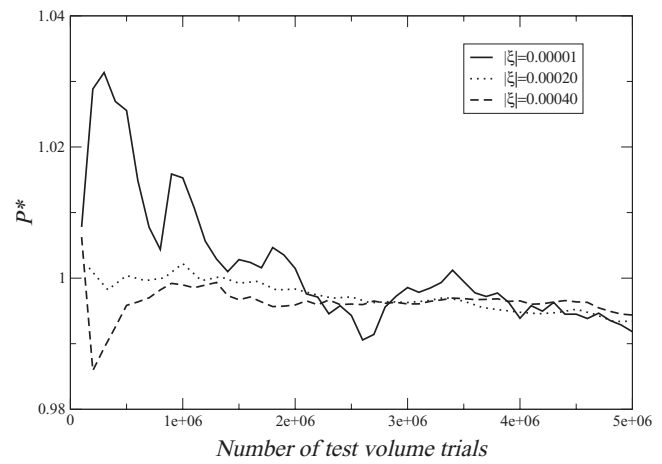


FIG. 3. Pressure, $P^* = \rho\sigma^3/k_B T$, as a function of the number of configurations used for its calculation, taking a configuration every simulation cycle. We performed simulations with $N = 1024$ 3-mer SW chains, at a density $\rho^* = 0.2215$ and at a supercritical temperature $T^* = 2.5$. These results were obtained from MC-NVT + VP simulations for the system in an elongated simulation cell, “Box 2,” and the corresponding pressure is $P^* = 1.0$, according to MC-NPT simulations. The VP method was applied using Eq. (33) for the pressure components and then pressure is given by $P^* = (p_{xx}^* + p_{yy}^* + p_{zz}^*)/3$, for different values of the volume perturbation parameter, $|\xi| = |\Delta V|/V$. The curves correspond to $|\xi| = 1 \times 10^{-5}$, $|\xi| = 20 \times 10^{-5}$, and $|\xi| = 40 \times 10^{-5}$. Such virtual volume changes cause non-overlapping configurations in 91%, 15%, and 2% of the attempts, respectively. Other cases studied and not shown, $|\xi| = 5 \times 10^{-5}$, $|\xi| = 10 \times 10^{-5}$, and $|\xi| = 30 \times 10^{-5}$, behave similar to the $|\xi| = 20 \times 10^{-5}$ curve.

values in short proofs. In this study we used as criteria $|\xi|$ values associated to $\sim 50\%$ HB overlapping configurations.

Another aspect to test is the similarity between pressure components when the system is homogeneous and isotropic. In Fig. 4(a) we present the comparison between the three components, p_{xx}^* , p_{yy}^* , and p_{zz}^* at a supercritical temperature. It is clearly seen that as the number of configurations for averages increases, the three components of the pressure tend to agree each other. This behavior gives us information about the intrinsic precision of the volume perturbation method, since the deviation between components for a large number of configurations is related to the size of the system. In this way is possible to determine how many configurations are required for a good estimation of P^* . In Fig. 4(b) we present the averaged pressure over the three curves of Fig. 4(a) and we compare it with the pressure calculated with an isotropic volume change, P_{xyz}^* . Taking the average in this case is equivalent to improve the statistics of the method, since the calculation for the three components is independent. The isotropic volume change produces an oscillating behavior, and we are presenting here the worst case. Similar results were found for an elongated simulation cell, “Box 2,” for supercritical temperatures. In the following results, we performed anisotropic volume changes to calculate the pressure tensor, and then the pressure from the trace, as explained in Sec. II F.

In the simulations we verified the symmetry and additivity identities, expressed in Eqs. (34) and (35). The symmetry in the compression and expansion contributions for the SW interactions can be seen in Table II for several pressure values. The first column indicates the pressure to test. This pressure

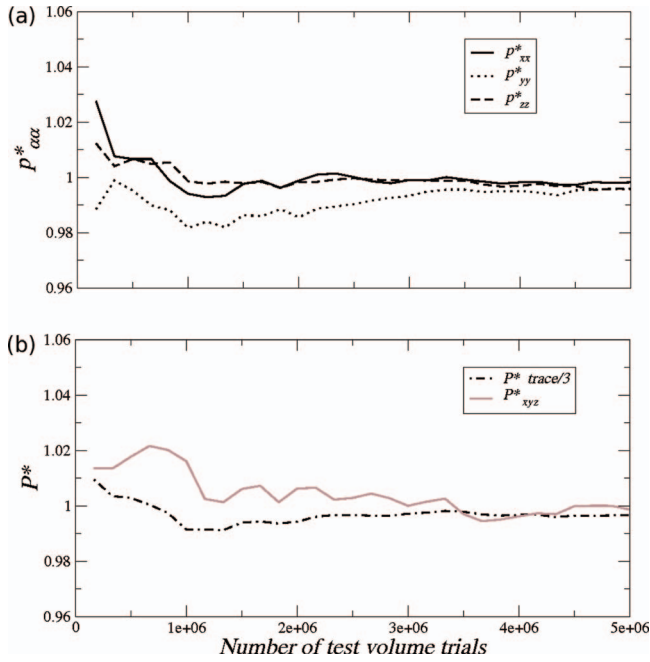


FIG. 4. (a) Pressure tensor, $p_{\alpha\alpha}^* = p_{\alpha\alpha}\sigma^3/k_B T$ where $\alpha = x, y, z$, as a function of the number of test volume trials, taking a configuration every simulation cycle. The volume perturbation method was applied using Eq. (36) and $|\xi| = 20 \times 10^{-5}$ to calculate the pressure components. (b) Comparison between the pressure values obtained using the pressure tensor components, $P^* = (p_{xx}^* + p_{yy}^* + p_{zz}^*)/3$, and the pressure calculated with an isotropic volume change, P_{xyz}^* , as a function of the test volume trials. In the second case, the volume perturbation parameter was $|\xi| = 20 \times 10^{-5}$, but the virtual volume change was applied to the three box dimensions at the same time. Similar behavior was observed for other cases, we show the worst correspondence between curves in the studied cases. All simulation results with $N = 1024$ 3-mer SW chains, at a density $\rho^* = 0.2215$ and at a supercritical temperature $T^* = 2.5$. These results were obtained in a cubic simulation cell, “Box 1,” and the corresponding pressure is $P^* = 1.0$, according to MC-NPT simulations.

was used to run a MC-NPT simulation to obtain the density average ρ^* for the system at equilibrium. The contributions from each perturbation and potential discontinuity were calculated from MC-NVT + VP simulations with Eqs. (16) and (32). These contributions and the weighted sum, Eq. (33), are also given in the same table. As can be seen, the comparison between $p_{-}^{*(SW)}$ and $p_{+}^{*(SW)}$ supports the symmetry identity given in Eq. (34). Accurate predictions also can be observed for a wide range of pressures. In the last column, the sum of

TABLE III. Pressure values for several thermodynamic states obtained from MC-NVT + VP simulations using Eq. (36) for a 3-mer SW chains system. The first column is the pressure to test, which was used to run a MC-NPT simulation to obtain the average density in equilibrium, ρ^* , given in column 2. This value was the fixed density for MC-NVT + VP simulations and also corresponds to the ideal contribution to pressure. The third column gives the results for pressure contributions calculated by compression, which includes the complete potential, $p_{-}^{*(HB+SW)}$. The fourth column gives the results for pressure contributions calculated by expansion, where only HB discontinuity accounts, $p_{+}^{*(HB)}$. Finally, last column shows the pressure calculated from Eq. (36). Simulation conditions were the same as in Table II.

P^* (NPT)	ρ^*	$p_{-}^{*(HB+SW)}$	$p_{+}^{*(HB)}$	P^* [Eq. (36)]
0.1	0.0992	0.013(2)	-0.0139(2)	0.098(2)
0.5	0.1911	0.373(3)	-0.0656(8)	0.499(4)
1.0	0.2215	0.881(5)	-0.1061(6)	0.996(6)
1.5	0.2390	1.414(9)	-0.142(2)	1.51(1)

the compression contributions are given, which will be used to verify Eq. (35).

Similar to Table II, the results for the same system and thermodynamic states using Eq. (36) are reported in Table III. The first two columns are the same as in Table II. The third column gives the compression contribution taking into account the complete interaction, $p_{-}^{*(HB+SW)}$, and the fourth column gives the expansion contribution, which includes only HB interactions, $p_{+}^{*(HB)}$. The third column of Table III and the last column of Table II are in very good agreement, indicating that the compression contribution also follows the additivity of the pressure as a consequence of the additivity of the potential. This supports the identity given in Eq. (35).

B. Other systems

Once the criteria to select the parameters method have been established, it is possible to study other systems. In Table IV we present the results for spherocylinders interacting via a SW potential (SWSC), with $\lambda = 1.5\sigma$ and $\epsilon = -1.0$. The expected pressure, $P^* = p\sigma^3/k_B T$, and its corresponding equilibrium density, ρ^* , are given in the first and second columns.^{34,35} The pressure contributions from compression and expansion, $p_{-}^{*(HB+SW)}$ and $p_{+}^{*(SW)}$, respectively, correspond to the third and fourth columns. The total pressure calculated from Eq. (36) is given in the last column. The results are in good agreement with the expected values for isotropic (I) and nematic (N) phases, as in the case of pressure P^*

TABLE II. Pressure values for several thermodynamic states obtained from MC-NVT + VP simulations using Eq. (33) for a 3-mer SW chains system. The first column is the pressure to test, which was used to run a MC-NPT simulation to obtain the average density in equilibrium, ρ^* , given in column 2. This value was the fixed density for MC-NVT + VP simulations and also corresponds to the ideal contribution to pressure. The columns 3 to 6 give the results for pressure contributions from compression and expansion calculated for each potential discontinuity, using Eqs. (16) and (32). Column 7 gives the pressure calculated from Eq. (33) and the last column shows the sum of the compression contributions. We performed simulations with $N = 1024$ molecules in a cubic simulation cell, “Box 1,” at a supercritical temperature of $T^* = 2.5$. The VP method was applied using $3-5 \times 10^6$ configurations for averages, taking a configuration every cycle. The value of the volume perturbation parameter, $|\xi|$, was chosen to get around 30%–50% of non-overlapping configurations for each case.

P^* (NPT)	ρ^*	$p_{-}^{*(HB)}$	$p_{+}^{*(HB)}$	$p_{-}^{*(SW)}$	$p_{+}^{*(SW)}$	P^* [Eq. (33)]	$p_{-}^{*(HB)} + p_{-}^{*(SW)}$
0.1	0.0992	0.272(2)	-0.0139(2)	-0.2585(6)	-0.2587(5)	0.098(2)	0.013(2)
0.5	0.1911	1.276(2)	-0.0657(8)	-0.903(1)	-0.902(2)	0.498(4)	0.373(3)
1.0	0.2215	2.043(7)	-0.1067(7)	-1.164(4)	-1.161(2)	0.99(1)	0.88(1)
1.5	0.2390	2.71(1)	-0.142(1)	-1.296(2)	-1.297(2)	1.51(2)	1.41(1)

TABLE IV. Pressure values for several thermodynamic states obtained from MC-NVT + VP simulations using Eq. (36) for a SW spherocylinders system (SWSC). We performed simulations with $N = 1020$ molecules in a cubic simulation cell, at reduced temperature $T^* = 5.0$. The VP method was applied to 4 groups of independent simulations, each one with 8×10^5 configurations for averages, taking a configuration every 10 simulation cycles. The value of the volume perturbation parameter, $|\xi|$, was chosen to get around 30%–50% of non-overlapping configurations for each case. The meaning of the columns is the same as in Table III.

P^* (NPT)	ρ^*	$p_{-}^{*(HB+SW)}$	$p_{+}^{*(HB)}$	P^* [Eq. (36)]
0.1	0.0359	0.0761(2)	-0.0113(1)	0.1008(3)
0.5	0.0698	0.499(1)	-0.0691(4)	0.500(2)
1.0	0.0876	1.043(2)	-0.1358(9)	0.995(3)
1.5	0.1041	1.56(1)	-0.17(1)	1.49(2)
1.75	0.1187	1.714(8)	-0.103(3)	1.73(1)

= 1.5, but the prediction deteriorates for smectic (SmA) phases, as can be seen for pressure $P^* = 1.75$. The pressure tensors for I, N, and SmA phases are given in Table V. The contributions from compression and expansion seem to be sensitive to the anisotropy of the system, as reported in the same table.

Another interesting case occurs when we add another discontinuity to the potential. In Table VI we show the results for 3-mer chains interacting via a square-shoulder plus a square-well potential (SS + SW). The parameters used were $\lambda_1 = 1.4\sigma$, $\epsilon_1 = 0.5$ for the shoulder and $\lambda_2 = 1.7\sigma$ and $\epsilon_2 = -1.0$ for the attractive segment. MC-NVT simulations with the volume perturbation method were carried out with $N = 1024$ spherocylinders at $T^* = 3.0$ and fixed ρ^* values in a cubic cell. In this case, the compression contribution includes the complete potential, $p_{-}^{*(HB+SS+SW)}$, while only HB

TABLE V. Pressure tensor for several thermodynamic states obtained from MC-NVT + VP simulations using Eq. (36) for a system of $N = 1020$ SW spherocylinders. The simulation details are the same as described in the Table IV and the first two columns have the same meaning. At the right side of the table, we show the results for compression (with HB+SW interactions), expansion (only HB interactions), and total pressure, obtained from anisotropic virtual volume changes. We compare the behavior of the components for the system at different phases, using the order parameter S , defined as the average of the second order Legendre polynomial of the angle between two particles. For pressures $P^* = 1.0$, $P^* = 1.5$, and $P^* = 1.75$ the phases are isotropic (I, $S = 0.05$), nematic (N, $S = 0.71$), and smectic A (SmA, $S = 0.93$), respectively. For the N and SmA phases the average director is $(n_x, n_y, n_z) = (-0.0537, 0.2224, 0.9735)$ and $(n_x, n_y, n_z) = (0.3221, 0.3063, 0.8958)$, respectively.

P^* (NPT)	ρ^*	Phase	p_{xx}^{*-}	p_{yy}^{*-}	p_{zz}^{*-}
1.0	0.0876	I	1.043(2)	1.042(3)	1.044(2)
1.5	0.1041	N	1.498(8)	1.53(1)	1.656(9)
1.75	0.1187	SmA	1.696(6)	1.694(9)	1.753(8)
			p_{xx}^{*+}	p_{yy}^{*+}	p_{zz}^{*+}
1.0	0.0876	I	-0.1358(9)	-0.136(1)	-0.1354(8)
1.5	0.1041	N	-0.107(7)	-0.14(1)	-0.26(1)
1.75	0.1187	SmA	-0.082(3)	-0.083(3)	-0.143(2)
			P_{xx}^*	P_{yy}^*	P_{zz}^*
1.0	0.0876	I	0.995(3)	0.993(4)	0.996(3)
1.5	0.1041	N	1.49(1)	1.49(3)	1.50(2)
1.75	0.1187	SmA	1.732(9)	1.73(1)	1.73(1)

TABLE VI. Pressure values for several thermodynamic states obtained from MC-NVT + volume perturbation simulations using Eq. (36) for a 3-mer SS + SW chains system. The system consisted of 3-mer chains with a hard core and a square-shoulder repulsive interaction plus a square-well attractive potential (HB + SS + SW). We performed simulations with $N = 1020$ molecules in a cubic simulation cell, at reduced temperature $T^* = 3.0$. The volume perturbation method was applied to 4 groups of independent simulations, each one with 1×10^6 configurations for average, taking a configuration every 10 simulation cycles. The value of the volume perturbation parameter, $|\xi|$, was chosen to get around 30%–50% of non-overlapping configurations for each case. The meaning of the columns is the same as in Tables III and IV.

P^* (NPT)	ρ^*	$p_{-}^{*(HB+SS+SW)}$	$p_{+}^{*(HB)}$	P^* [Eq. (36)]
0.1	0.0702	0.0329(4)	-0.00307(5)	0.1000(5)
0.5	0.1436	0.379(2)	-0.0211(2)	0.502(2)
1.0	0.1752	0.868(2)	-0.0434(4)	1.000(3)
1.5	0.1952	1.379(5)	-0.0676(7)	1.507(6)

discontinuity accounts for expansion calculation, $p_{+}^{*(HB)}$. The total pressure was calculated as proposed in Eq. (39). As can be seen, the results are in good agreement with the expected values.

In all the systems studied in this work (SW trimer, SWSC, and SS + SW trimer) it was observed that the pressure value is overestimated by around 10%–13% when only compression is included in the virtual volume perturbation. This was also observed by Brumby *et al.* in convex HB systems.¹⁵

C. Surface tension

Finally, we present results for the calculation of the surface tension using the volume perturbation method for discontinuous potentials. We used the system of 3-mer SW chains in an elongated box (“Box 2”) that required a larger number of configurations than in the homogeneous cases, as described in Sec. III C. In Figure 5 we present the pressure components for this system at temperature $T^* = 1.1$, and a similar qualitative behavior was observed for other temperatures.

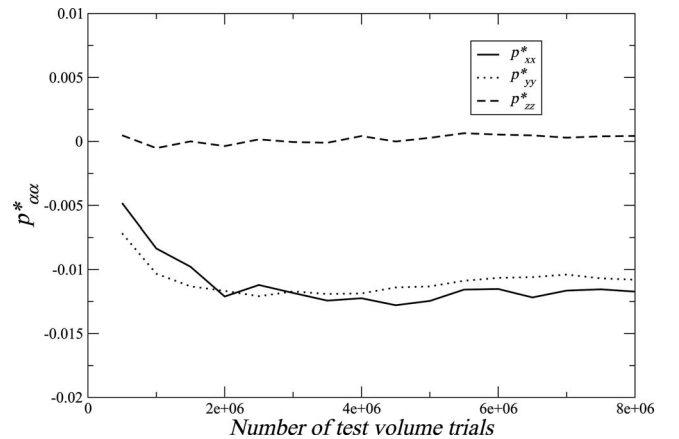


FIG. 5. Pressure tensor, $p_{\alpha\alpha}^* = p_{\alpha\alpha}\sigma^3/k_B T$ where $\alpha = x, y, z$, as a function of the number of test volume trials. We performed direct coexistence simulations with $N = 1024$ 3-mer SW chains in an elongated simulation cell, “Box 2,” at subcritical temperatures. The volume perturbation method was applied to 8 groups of independent simulations, each one with 8×10^6 configurations for averages, taking a configuration every cycle. The graphic corresponds to $T^* = 1.1$ and similar qualitative behavior was presented by the results for other temperatures.

TABLE VII. Pressure tensor and surface tension, $\gamma^* = \gamma\sigma^2/k_B T$, obtained from MC-NVT + VP simulations using Eq. (36) for a 3-mer SW chains system. The first column is the reduced temperature, which corresponds to subcritical values. The second to fourth columns give the reduced pressure tensor. Column 5 corresponds to the vapor pressure calculated from a fit to MC-NPT simulations data, as described in Sec. III C. Column 6 shows the surface tension results that were obtained using as the normal component p_N^* , the pressure component p_{zz}^* , which was calculated directly from the MC-NVT + VP simulations. The last column shows the surface tension results that were obtained using as the normal component, p_N^* , the vapor pressure calculated independently (column 5). We performed direct coexistence simulations with $N = 1024$ molecules in an elongated simulation cell, “Box 2,” at subcritical temperatures. The volume perturbation method was applied to 8 groups of independent simulations, each one with 8×10^6 configurations for averages, taking a configuration every cycle.

T^*	p_{xx}^*	p_{yy}^*	p_{zz}^*	p_V^*	$\gamma^* (p_N^* = p_{zz}^*)$	$\gamma^* (p_N^* = p_V^*)$
1.1	$-1.17(7) \times 10^{-2}$	$-1.08(6) \times 10^{-2}$	$4(6) \times 10^{-4}$	$1.5(6) \times 10^{-4}$	0.58(6)	0.57(4)
1.2	$-8.0(7) \times 10^{-3}$	$-6.4(7) \times 10^{-3}$	$1.3(8) \times 10^{-3}$	$6.5(7) \times 10^{-4}$	0.42(7)	0.40(4)
1.3	$-5.0(4) \times 10^{-3}$	$-4.2(7) \times 10^{-3}$	$1.2(5) \times 10^{-3}$	$1.7(1) \times 10^{-3}$	0.29(5)	0.32(3)
1.4	$-7(6) \times 10^{-4}$	$-2(4) \times 10^{-4}$	$3.0(4) \times 10^{-3}$	$3.5(1) \times 10^{-3}$	0.17(4)	0.20(3)

As can be seen in Figures 1(a) and 1(e), the $T^* = 1.1$ state has few molecules in the gas phase, which causes a very low normal pressure. The numerical results for this and other states are presented in Table VII. From second to fourth columns, the calculated components are given. The fifth column corresponds to the vapor pressure calculated by independent MC-NPT simulations. The last two columns give the results for surface tension calculated with Eq. (41) for two cases: (1) using as normal component the calculated from volume perturbation, $p_N^* = p_{zz}^*$; and (2) using as normal component the calculated from the independent MC-NPT simulation $p_N^* = p_V^*$.

By increasing the temperature, more molecules migrate to the gas (see Figure 1) and then the prediction for the normal component p_{zz}^* improves in precision and accuracy. This can be noticed because the relative error is lower for higher temperatures, and this component is closer to the vapor pressure value obtained from MC-NPT simulations. The tangential components, p_{xx}^* and p_{yy}^* , are lowered as the temperature increases. When the values are of the order of 10^{-4} , the results are not reliable, since they are of the same order of magnitude than the intrinsic error of the method. It appears that the final value of the surface tension is not affected in the calculation, and the results using $p_N^* = p_{zz}^*$ and $p_N^* = p_V^*$ are very similar. The surface tension values decrease when the temperature increases, as expected.

V. CONCLUSIONS

An extension of the test volume perturbation method has been developed in order to obtain the pressure and surface tension of non-spherical molecules interacting via discontinuous potentials, in a single simulation. We studied specific models such as total flexible chain molecules formed by tangent spheres interacting via SW and SS + SW potentials, and SW spherocylinders. According to the theoretical modeling, the pressure contribution arising from the repulsive interaction is asymmetric for the infinite energy case, whereas for finite attractive and repulsive interactions there is a symmetry with respect to expansion or contraction of the simulation cell. Pressure contributions keep the additivity of the potential interactions. These two properties allow us to give a simplified expression for the pressure of the non-spherical systems. We found that, in order to reduce significantly the uncertainty

of the surface tension, longer runs are required. In summary, to evaluate a certain component of the pressure tensor for a molecular system having both hard and finite discontinuous (attractive and/or repulsive) contributions, all what is needed is: (1) to perform a test volume where one of the lengths of the simulation box is reduced, (2) to compute the energy change of this contraction using the original total intermolecular potential, and (3) to add the hard body contribution that arises on expansion. If this procedure is applied, the correct result is obtained, regardless of whether atomic or molecular fluids are used.

Our results agree with NPT simulations for bulk pressure values; some problems due to temperature are observed when the pressure tensor is obtained in coexisting phases. Even when we took care in avoiding size-system effects using a cross sectional area of around $(12\sigma)^2$, a more detailed study is required for complex molecules, such as spherocylinders or long-chain molecules.

ACKNOWLEDGMENTS

This work was supported under CONACYT (México) Grant No. 61418 and a Becas Mixtas Scholarship (G.J.S.). We also acknowledge support from MEC (Spain), through Grant No. FIS2010-16159.

- ¹J. G. Kirkwood and F. P. Buff, *J. Chem. Phys.* **17**, 338 (1949).
- ²L. L. Lee, *Molecular Thermodynamics of Non-ideal Fluids* (Butterworth, Boston, 1988).
- ³J. S. Rowlinson and B. Widom, *Molecular Theory of Capillarity* (Oxford University Press, Oxford, 1989).
- ⁴L. D. Landau and E. M. Lifschitz, *Theory of Elasticity*, 3rd ed. (Butterworth-Heinemann, Oxford, 1986).
- ⁵E. Salomons and M. Mareschal, *J. Phys.: Condens. Matter* **3**, 3645 (1991).
- ⁶F. del Río, *Mol. Phys.* **76**, 21 (1992).
- ⁷F. del Río and A. Gil-Villegas, *Mol. Phys.* **77**, 223 (1992).
- ⁸W. Zwanzig, *J. Chem. Phys.* **22**, 1420 (1954).
- ⁹R. Eppenga and D. Frenkel, *Mol. Phys.* **52**, 1303 (1984).
- ¹⁰V. I. Harismiadis, J. Vorholz, and A. Z. Panagiotopoulos, *J. Chem. Phys.* **105**, 8469 (1996).
- ¹¹H. L. Vörtler and W. R. Smith, *J. Chem. Phys.* **112**, 5168 (2000).
- ¹²G. J. Gloor, G. Jackson, F. J. Blas, and E. de Miguel, *J. Chem. Phys.* **123**, 134703 (2005).
- ¹³E. de Miguel and G. Jackson, *J. Chem. Phys.* **125**, 164109 (2006).
- ¹⁴E. de Miguel and G. Jackson, *Mol. Phys.* **104**, 3717 (2006).
- ¹⁵P. E. Brumby, A. J. Haslam, E. de Miguel, and G. Jackson, *Mol. Phys.* **109**, 169 (2011).

- ¹⁶J. M. Míguez, M. M. Piñeiro, A. I. Moreno-Ventas Bravo, and F. J. Blas, *J. Chem. Phys.* **136**, 114707 (2012).
- ¹⁷C. Vega and E. de Miguel, *J. Chem. Phys.* **126**, 154707 (2007).
- ¹⁸J. M. Míguez, D. González-Salgado, J. L. Legido, and M. M. Piñeiro, *J. Chem. Phys.* **132**, 184102 (2010).
- ¹⁹J. G. Sampayo, F. J. Blas, E. de Miguel, E. A. Müller, and G. Jackson, *J. Chem. Eng. Data* **55**, 4306 (2010).
- ²⁰F. J. Blas, L. G. MacDowell, E. de Miguel, and G. Jackson, *J. Chem. Phys.* **129**, 144703 (2008).
- ²¹L. G. Macdowll and P. Bryk, *Phys. Rev. E* **75**, 61609 (2007).
- ²²E. de Miguel, *J. Phys. Chem. B* **112**, 4674 (2008).
- ²³A. Ghoufi and P. Malfreyet, *J. Chem. Phys.* **136**, 24104 (2012).
- ²⁴K. Binder, *Phys. Rev. A* **25**, 1699 (1982).
- ²⁵J. J. Potoff and A. Z. Panagiotopoulos, *J. Chem. Phys.* **112**, 6411 (2000).
- ²⁶J. R. Errington and D. A. Kofke, *J. Chem. Phys.* **127**, 174709 (2007).
- ²⁷G. A. Chapela, G. Saville, S. M. Thompson, and J. S. Rowlinson, *J. Chem. Soc., Faraday Trans. 2* **73**, 1133 (1977).
- ²⁸L. Chen, *J. Chem. Phys.* **103**, 10214 (1995).
- ²⁹M. González-Melchor, F. Bresme, and J. Alejandre, *J. Chem. Phys.* **112**, 104710 (2005).
- ³⁰P. Orea, J. López-Lemus, and J. Alejandre, *J. Chem. Phys.* **123**, 114702 (2005).
- ³¹J. D. Weeks, D. Chandler, and H. C. Andersen, *J. Chem. Phys.* **54**, 5237 (1971).
- ³²F. A. Escobedo and J. J. de Pablo, *Mol. Phys.* **87**, 347 (1996).
- ³³C. Vega and S. Lago, *Comput. Chem.* **18**, 55 (1994).
- ³⁴D. C. Williamson and F. del Río, *J. Chem. Phys.* **109**, 4675 (1998).
- ³⁵A. Cuetos, B. Martínez-Haya, L. F. Rull, and S. Lago, *J. Chem. Phys.* **117**, 2934 (2002).